

60 T pulsed magnetic field in Bitter magnet made of tungsten and coiled by liquid helium

Streszczenie. W artykule przedstawiono budowę magnesu Bittera przeznaczonego do wytwarzania silnych impulsowych pól magnetycznych i układu jego zasilania. Magnes składał się z pakietu płyt wykonanych z wolframu i był chłodzony ciekłym helem. Wykorzystano unikalną właściwość, polegającą na tym, że wolfram w temperaturze kilku stopni Kelvina nie przechodzi w stan nadprzewodnictwa, ale wykazuje niezwykle niską rezystywność rzędu $10^{-13} \Omega\text{m}$. Dlatego taki magnes wymaga bardzo małej mocy zasilania i nie ma ograniczenia wartości indukcji przez pole krytyczne. Opisano działanie tego układu i sposób pomiaru indukcji wytworzonego pola magnetycznego. Osiągnięto impulsy o maksymalnej indukcji 60 T i czasie trwania 2 μs . (**Impulsowe pole magnetyczne 60 T w magnesie Bittera chłodzonym ciekłym helem**)

Abstract. This paper describes the construction of a Bitter magnet intended for generating high pulsed magnetic fields, along with its corresponding power supply system. The magnet was constructed using a tungsten plate stack and was cooled with liquid helium. This design capitalized on the distinctive characteristic of tungsten, which does not transition into a superconducting state at temperatures within a few Kelvin, while simultaneously exhibiting an exceptionally low resistivity on the order of $10^{-13} \Omega\text{m}$. Therefore, this magnet necessitates a significantly low-power supply and is not constrained by the critical field when it comes to the induction value. The functioning of this system, along with the technique employed for measuring the induction of the resulting magnetic field, is elucidated. This setup successfully achieved pulses with a maximum induction of 60 T and a duration of 2 μs . (**Impulsowe pole magnetyczne o indukcji 60 T w magnesie Bittera wykonanym z wolframu i chłodzonym ciekłym helem**)

Słowa kluczowe: magnes Bittera, pole magnetyczne, impuls, rezystywność, ciekły hel, chłodzenie.

Keywords: Bitter magnet, magnetic field, impulse, resistivity, liquid helium, cooling.

Introduction

A magnetic field is a physical object commonly found throughout the Universe. The values of induction of naturally produced magnetic fields are in the range 10^{-18} - 10^{14} T. The highest magnetic fields are produced by neutron stars and magnetars [1]. Even stronger magnetic fields of 10^{40} T induction are considered in theoretical investigations, which may have existed in the early evolution of the Universe. Within these magnetic fields, it is plausible that the Grand Unification Theory (GUT) takes place [2]. On the other end of the spectrum, the weakest magnetic fields originate from certain nanoparticles and organs within living organisms, including the brain [3, 4]. To measure such fields, superconducting quantum interference devices (SQUID) and atomic magnetometers are employed [5, 6].

Magnetic fields find extensive applications in various domains of technology and scientific research. One notable example is their utilization in directing and focusing particle beams within accelerators, as well as in the containment of plasma for controlled thermonuclear fusion investigations [7-9]. Moreover, remarkable quantum phenomena, such as the quantum Hall effect, manifest exclusively in the presence of strong magnetic fields and extremely low temperatures [10]. Consequently, magnetic fields are artificially generated through technical means. In laboratory settings, the upper limit for stationary magnetic fields typically ranges between 50-60 T [11-13]. For pulsed magnetic fields, this limit reaches 2700 T. The duration of a pulse of maximum j induction is of the order of 10^{-6} s. Attaining such high magnetic fields is exclusively achieved through the utilization of explosive magnetic flux compression techniques, albeit at the cost of significantly compromising the integrity of the experimental system's components [14-16].

The generation of robust magnetic fields with inductions exceeding 5 T necessitates overcoming numerous technical challenges. The foremost among these challenges include the provision of high electric currents on the order of kA or even MA, the construction of coils with low electrical resistance and exceptional mechanical strength, as well as the implementation of rapid cooling mechanisms [17].

Consequently, in addition to conventional devices like Bitter coils, polyhelical coils, superconducting coils, hybrid coils (often referred to as magnets), and single coils, researchers are actively seeking new technical solutions [18-21].

One innovative solution is to use an accelerated electron beam in a linear accelerator to generate strong pulsed magnetic fields. The duration of the pulses of the generated field is extremely short at 10^{-12} s [22, 23]. The electrons passed through the sample made of cobalt and caused it to become permanently magnetised. The resulting boundaries of the magnetic domains were subsequently examined using microscopy techniques. The authors of the referenced papers suggest that investigating the rapid magnetization of materials in such a short timeframe holds potential significance for the advancement of novel approaches in rapid information storage methods.

The micro-coil serves as a notable example of an innovative solution enabling the production of pulsed magnetic fields characterized by an induction of 50 T and a duration of 30 ns [24]. This magnetic field is generated within a microcoil featuring an aperture radius of 50 μm . The microcoil was a single coil made of copper deposited on a silicon wafer, covered with an insulating layer of SiO_2 . The outer radius of this coil was 150 μm , its thickness 10 μm . A maximum current of 4 kA was generated by discharging a 12 nF capacitor bank. The coil, along with its accompanying bank, had dimensions measuring several centimetres, while the entire circuit could fit comfortably in the palm of one's hand. Notably, this circuit operated at room temperature, enabling the generation of magnetic field pulses repeatedly without compromising the integrity of the coil. Despite the extremely small size of the microcoil and the production of a magnetic field in a volume of only $78.5 \cdot 10^{-5} \text{ mm}^3$, the circuit enabled the study of the magneto-optical Faraday effect.

This article outlines the development of a small-sized Bitter magnet made of tungsten and cooled by liquid helium, enabling the generation of powerful pulsed magnetic fields. Tungsten at a liquid helium temperature of 4.2 K does not go into a superconducting state, but exhibits the unique property of decreasing its resistivity to an extremely small value $\rho_w = 2.67 \cdot 10^{-13} \Omega\text{m}$. This value is much smaller than

the resistivity of other metals at this temperature, which for example for copper is $\rho_m = 2 \cdot 10^{-11} \Omega m$. [25, 26]. The advantage of a coil made of tungsten is the low amount of heat generated when a strong electric current flows. A second advantage of this material is its high tensile strength.

Experimental setup

The system employs a Bitter magnet made of tungsten, which essentially takes the form of a specialized coil with a unique design [27]. The coil structure is shown in Fig. 1, wherein a stack of identically shaped ring-like plates 1 is arranged. Each plate features a central hole 2 and radial intersections 3, while being rotated in relation to adjacent plates. Insulating spacers 4 of matching shape are positioned between the plates to maintain separation. Consequently, the plates converge at the surface 5 in the form of a ring slice, creating a spiral configuration that allows for the passage of an electric current. A useful magnetic field is generated in the central hole of the plates with radius r_w . Furthermore, the plates 1 and insulating spacers 2 feature symmetrically positioned holes 6 to facilitate the circulation of coolant, while additional holes 7 have been incorporated to accommodate screws for compressing the assembly in the axial direction. This coil design provides high strength and good cooling conditions. The experimental setup used a stack composed of $n = 33$ plates 1, made of tungsten sheet of thickness $g_1 = 1$ mm. Insulating spacers 2 with a thickness of $g_2 = 0.1$ mm, made of glass fibre reinforced polyester film, were placed between the plates. The outer radius of the plates and spacers was $r_z = 50$ mm and the radius of the central hole was $r_w = 3$ mm. Each plate exhibited a total of 160 symmetrically distributed holes with a diameter of 2 mm, intended specifically for the passage of liquid helium. In addition, there were 10 holes of 6.2 mm diameter in each plate for the packet compression screws, which were located near the outer edge of the plate. The filling factor of the stack, calculated as the ratio of the volume of the electrically conductive part of the stack to the entire volume of the package, was $\lambda = 0.81$. The entire volume of the stack was calculated as the volume of a hollow cylinder with radii r_z , r_w and a height equal to the sum of the thicknesses of the plates and insulating spacers, i.e. 36.2 mm.

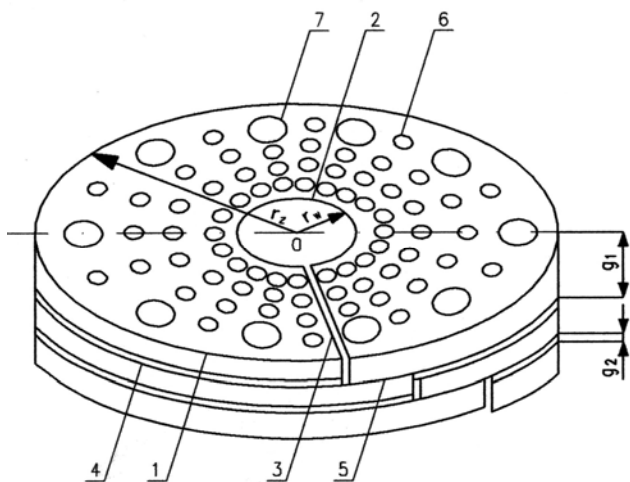


Fig. 1. Method of arranging the plates in a Bitter magnet; 1 – plate made of tungsten, 2 – cutting, 3 – insulating spacer made of polyester film, 4 – contact surface of the plates, 5, 6 – holes for cooling with liquid helium and for screws, respectively, r_w , r_z – radii of the working hole and the outer radius of the plate, respectively, g_1 , g_2 – thicknesses of the plate and the insulating spacer, respectively

The plate stack 1, referred to as a Bitter magnet and designated as "B" hereafter, was assembled within the cryostat presented in Fig. 2. The stack was positioned between two pressure plates 3, which were placed above and below it. These pressure plates shared the same radii and holes as the plates 1, but lacked radial intersections. They made direct contact with the outermost plates of the stack. Through the holes in the stack and pressure plates 3 were bolts 5, onto which insulating sleeves 6 were applied and nuts 7 were screwed in. In addition, one power cable 8, made of copper rod with a diameter of 10 mm, was connected to each pressure plate. The power wires were connected using the nuts on the clamping screws. To ensure optimal contact, the end of each wire was flattened. The plate stack was then immersed in liquid helium 9, filling a cryostat comprised of an inner shell 10 and an outer shell 11. Between these shells, a 50 mm thick thermal insulation layer 12 made of porous polyurethane was incorporated. The cryostat was supported by attachments 13 fixed to the outer shell 11. Additionally, the top cover of the cryostat featured two filler tubes 14 for the introduction of liquid helium and the release of its vapours. The bottom of the cryostat was connected to a drain pipe 15 sealed by a valve 16. The cryostat consisted of inner and outer shells made of austenitic steel, which remained non-magnetized. The plate 1 stack was isolated from the bottom of the cryostat. The power feed lines 8 were led outside the cryostat through insulating grommets 18 made of Teflon. The central hole of the plate package aligned with the cryostat axis and housed a working tube 19 made of Teflon. This tube, with an inner diameter of 2 mm, served as the area for generating the useful magnetic field.

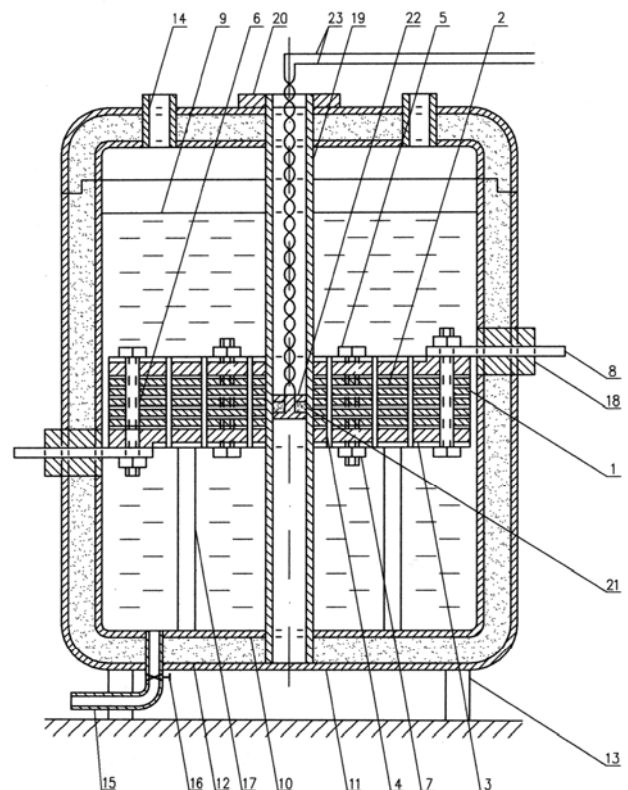


Fig. 2. Structure of the Bitter magnet cryostat shown in axial section; 1 – tungsten plate, 2 – insulating spacer, 3 – pressure plate, 4 – liquid helium cooling hole, 5 – screw, 6 – insulating sleeve, 7 – nut, 8 – supply line, 9 – liquid helium, 10, 11 – cryostat shells respectively: inner and outer, 12 – thermal insulation layer, 13 – cryostat support, 14 – filling tube, 15 – drain tube, 16 – drain valve, 17 – stack supports, 18 – insulation bushing, 19 – working tube, 20 – ring, 21 – measuring coil, 22 – coil bobbin, 23 – wires

The internal dimensions of the cryostat were as follows: diameter 200 mm and height 250 mm. The capacity of the cryostat was 7.85 dm^3 . The initial cooling process of the Bitter magnet from ambient temperature was conducted in two distinct stages. The first stage involved cooling from approximately $22\text{-}25^\circ\text{C}$ to a temperature of -195°C , which corresponds to the boiling point of liquid nitrogen. The second stage entailed further cooling from -195°C to the boiling point of liquid helium at -268.8°C (4.2 K). This two-stage approach was implemented to minimize the consumption of liquid helium, thus ensuring an economical operation. Upon completion of the first cooling stage, the drain valve 16 was opened, allowing the removal of liquid nitrogen from the cryostat. Subsequently, the cryostat was promptly filled with liquid helium through one of the inlet tubes 14. The first cooling stage necessitated the evaporation of 6 litres of liquid nitrogen, while the second stage required 24 litres of liquid helium.

To determine the induction of the magnetic field generated, a measuring coil 21 was used, wound on a bobbin 22 in the shape of a cylinder with a groove on the circumference and placed inside a tube 19. The coil consisted of $n_c = 2$ turns of copper wire with a diameter $d_d = 0.2 \text{ mm}$. The outer diameter of the coil was $d_c = 2 \text{ mm}$. The bobbin, along with the coil, was adjustable along the tube 19 and could be fixed at a desired distance from the centre of the plate stack to measure the magnetic field induction at that specific position. The ends of the coil were connected using copper wires 23, which were then led outside the cryostat. The diameter of the wires matched that of the coil wire. The total length of the wires was 1.5 m and their resistance including the coil was $R_p = 0.817 \Omega$. To mitigate interference from induced voltages in the pulsed magnetic field, the wires were twisted together. This twisting helps reduce the impact of voltages that can be induced in wires positioned within a pulsed magnetic field.

The Bitter B magnet housed within the cryostat was integrated into a circuit, as illustrated by the schematic diagram depicted in Fig. 3. The circuit incorporated a capacitor bank C with a capacitance of 0.34 nF. To minimize resistance in the connections between the capacitors and enable the efficient flow of high current, custom-designed flat capacitors were employed. These capacitors, featuring a capacitance of 0.085 nF each, were connected in parallel using 2.5 mm copper wires. The capacitor covers were square-shaped, measuring 48 mm on each side, and were fashioned from aluminium sheet material. The gap between the covers was 5 mm wide and was filled with a plate made of Teflon with a relative dielectric permeability of $\epsilon_r = 2.1$. To charge the capacitors, a DC power supply S was employed. The power supply was connected to the bank and charged the capacitors by means of a switch W throughout the charging process.

The capacitor bank C was linked to the Bitter magnet via an ionization ignitron Z. The ignitron was composed of a quartz glass tube housing two flat tungsten electrodes. These electrodes were positioned within the tube, with a gap of 2 mm separating them. The tube was filled with a mixture of argon and sulphur hexafluoride SF_6 at atmospheric pressure. The SF_6 content accounted for 70% of the mixture volume. This was similar to the arrangement used for pulsed magnetic field generation using a microcoil [24]. To activate the ignitron, a 2 W semiconductor laser D emitting blue light with a wavelength of 450 nm was utilized. A focusing lens F was employed to concentrate the laser beam inside the ignitron tube. The focused beam caused a localized temperature increase, leading to the ionization of the gas mixture present within the ignitron. Consequently, the gas mixture within the ignitron became electrically

conductive. The selection of gases and the specific composition of the mixture enabled the ignitron to conduct electricity only for the duration of the light pulse emitted by the laser. Rectangular voltage pulses, required to power the laser, were generated using a generator G connected to an amplifier A. The previously described measurement coil M (numbered 22 in Fig. 2) was connected to a voltage divider consisting of two resistors R_1 , R_2 , having resistances $R_1 = 3.3 \text{ k}\Omega$ and $R_2 = 82 \Omega$. The resistor R_2 was connected in parallel to the input of the digital oscilloscope. This arrangement allowed the induction ΔB of the magnetic field pulses produced by the Bitter magnet to be determined from the voltage changes recorded using the oscilloscope.

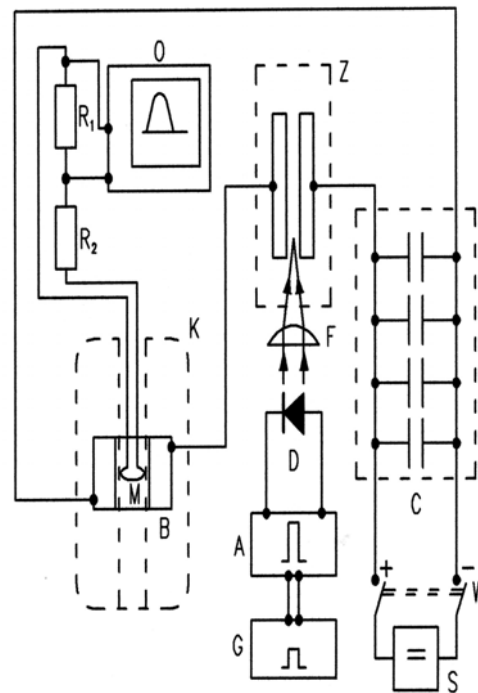


Fig. 3. Schematic of the experimental setup; B – Bitter magnet, K – cryostat, C – capacitor bank, S – power supply, W – switch, Z – ignitron, F – focusing lens, D – semiconductor laser, G – generator, A – amplifier, M – measuring coil, R_1 , R_2 – resistors, O – digital oscilloscope; maximum voltage $\Delta U_2 = 3.72 \text{ V}$

Results of experiments and discussion

The capacitor bank C was connected to the DC power supply S through switch W and charged to a maximum voltage $U_0 = 218 \text{ V}$. Once charged, the bank was disconnected from the power supply. A single rectangular voltage pulse of duration $\Delta t = 2 \mu\text{s}$ was then generated using generator G, which, after amplification, powered laser D. The light pulse emitted by the laser caused ignitron Z to conduct. Then capacitor bank C discharged and an electric current flowed through Bitter magnet B, which produced a pulsed magnetic field of maximum induction ΔB in the central hole of this magnet. The magnetic induction flux $\Delta \Phi$, penetrating through the measuring coil M produced an electromotive force E_1 in it and caused an electric current of intensity I_p to flow in a circuit consisting of the coil and resistors R_1 , R_2 . The voltage drop ΔU_2 on the resistor R_2 was observed on the screen of a digital oscilloscope. The measuring coil M was initially placed in the centre of the Bitter magnet. The recorded changes in the voltage drop ΔU_2 in this case are shown in Fig. 4. According to the designations adopted earlier, the absolute value of the electromotive force E_1 , induced in measuring coil M, is expressed by the following formula

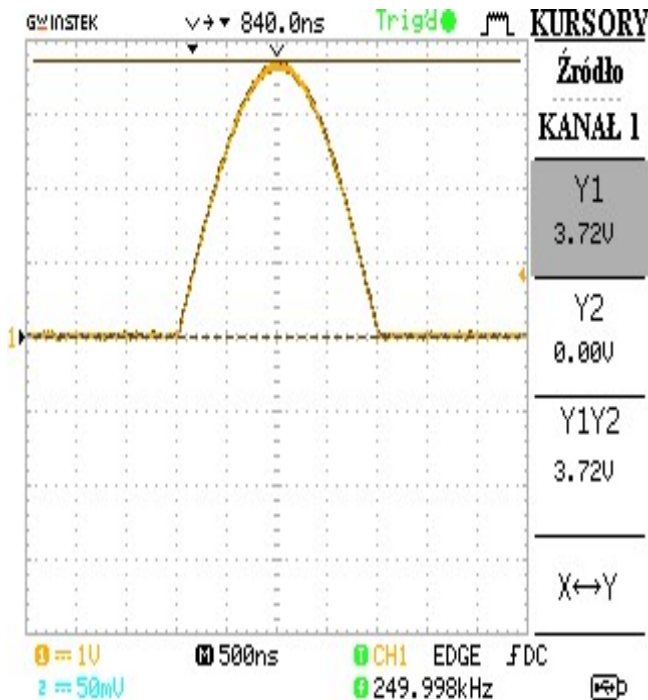


Fig. 4. Dependence of the voltage drop ΔU_2 on the resistor R_2 on the duration of the magnetic field pulse Δt for the measurement coil M placed in the centre of the Bitter magnet

$$(1) \quad E_1 = \frac{\Delta \Phi}{(\Delta t / 2)} = \frac{n_c (\pi d_c^2 / 4) \Delta B}{(\Delta t / 2)} = \frac{\pi n_c d_c^2 \Delta B}{2 \Delta t}$$

The voltage drop ΔU_2 at resistor R_2 can be calculated from the formula

$$(2) \quad \Delta U_2 = I_1 R_2 = \frac{E_1 R_2}{R_p + R_1 + R_2}$$

After substitution and transformation from equations (1) and (2), the equation is obtained

$$(3) \quad \Delta B = \frac{2(R_p + R_1 + R_2) \Delta U_2 \Delta t}{\pi n_c d_c^2 R_2} = k_B \Delta U_2 \Delta t$$

The proportionality factor k_B introduced in equation (3) depends only on the parameters of the measuring circuit. After substituting the previously given values of these parameters from equation (3), $k_B = 17.01 \cdot 10^6$ T/(Vs) was calculated. Knowing the value of this coefficient, as well as Δt and the maximum voltage $\Delta U_2 = 3.72$ V, as read from the oscilloscope, the maximum induction of the generated magnetic field ΔB can be calculated. Using the determined value of k_B and Fig. 4, $\Delta B = 63.1$ T was calculated. The uncertainty of the calculated value was estimated as ± 3.1 T i.e. $\pm 5\%$.

A tungsten plate package is a spiral with flat coils having inner radii r_w , outer radii r_z and coil thickness g_1 . The resistance of such a package R_w is expressed by the following formula

$$(4) \quad R_w = \frac{2\pi \rho_w}{g_1 \lambda \ln(r_z / r_w)}$$

After substituting the previously adopted values into equation (4), $R_w = 2.43 \cdot 10^{-8}$ Ω was obtained. The value mentioned is very small and has virtually no effect on the resistance of the entire RLC circuit, which governs the discharge of the capacitor bank C in the considered circuit.

As a result, the practical importance lies in the resistance of the other circuit elements, such as the wires feeding the stack, the wires connecting the capacitors, and the ignitron. These elements play a crucial role in the practical functioning of the circuit. This resistance was measured in the conduction state of the ignitron and was $R = 5.45 \cdot 10^{-3}$ Ω . The measured inductance of the entire circuit was $L = 1.19$ mH. The capacitance of the capacitor bank used, $C = 0.34$ nF, was chosen so that its discharge would take place at circuit resonance. The resonant oscillation period T is expressed by the well-known formula

$$(5) \quad T = 2\pi \sqrt{LC}$$

Using equation (5) and the previously stated values, $T = 4$ μ s is obtained. Therefore, the conduction time of the ignitron $\Delta t = 2$ μ s allowed one pulse of the magnetic field to be generated.

The relationship between the magnetic field induction ΔB , produced by the Bitter magnet, and the current supplied to it is expressed by the formula [28]

$$(6) \quad \Delta B = \mu_0 G(\alpha, \beta) \sqrt{\frac{I^2 R_w \lambda}{\rho_w r_w}}$$

where μ_0 – denotes the magnetic permeability of the vacuum, $G(\alpha, \beta)$ – Fabry function depending on the parameters expressing the size ratio of the magnet, it is: $\alpha = r/r_{zw}$, $\beta = l/(2r_w)$ and defined by the formula

$$(7) \quad G(\alpha, \beta) = \sqrt{\frac{1}{4\pi\beta \ln \alpha}} \ln \left(\frac{\beta + \sqrt{1 + \beta^2}}{\beta + \sqrt{\alpha^2 + \beta^2}} \right)$$

Based on the given values for $\alpha = 16.67$, $\beta = 6$, and $G(\alpha, \beta) = 0.1198$, and by performing the necessary transformations on equation (6), the current supplying the magnet was calculated to be $I = 39.93 \cdot 10^3$ A. For this current and the measured circuit resistance $R = 5.45 \cdot 10^{-3}$ Ω , the initial voltage to which the capacitor bank was charged $U_0 = 218$ V is obtained.

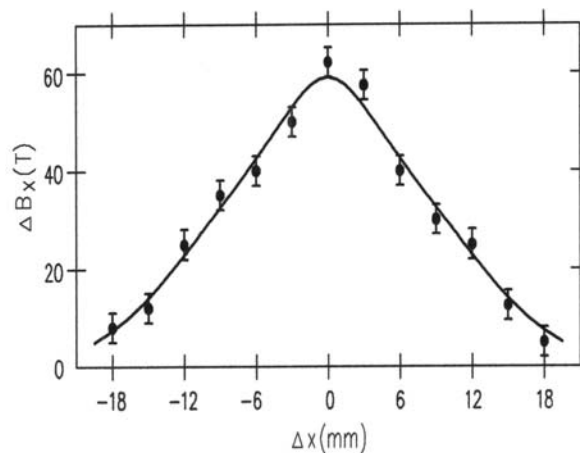


Fig. 5. Magnetic field induction ΔB_x on the axis of the Bitter magnet, as a function of distance Δx from its centre 0; the solid line shows the results of the calculation

In the subsequent stage of testing, the previously described method was employed to ascertain the maximum magnetic field induction along the axis of the Bitter magnet, specifically at points beyond its centre. To accomplish this, the measuring coil M was positioned at progressively

greater distances from the centre of the magnet. The distance between successive positions of the coil was $\Delta x = 3$ mm. The determined values of the magnetic field induction ΔB_x are shown in Fig. 5. The measured results were compared with calculations performed using a formula derived from the existing literature specifically for a Bitter magnet. This formula takes into account the assumption that the current density j in the plates decreases with distance r from the axis of the Bitter magnet directly proportional to $1/r$ [28]. Differences between measured results and calculated values do not exceed 10%.

Conclusions

The conducted tests successfully demonstrated the viability of utilizing liquid helium-cooled tungsten in the construction of Bitter magnets. This approach proved effective in generating powerful pulsed magnetic fields, all achieved through the utilization of limited technical resources. The volume of the magnetic field useful for testing in the magnet presented was about $8 \cdot 10^4$ times that of a microcoil [24]. This allows much larger sample sizes to be tested and facilitates measurements. Notable advantages of this approach include the exceptionally low power loss and the absence of limitations on magnetic induction imposed by the critical field, a constraint typically encountered in superconducting magnets. For comparison, if the same Bitter magnet were made of copper and operated at 20°C, its resistance would be $1.56 \cdot 10^{-3} \Omega$. Then the power lost as heat would be 2.5 MW, whereas for a magnet made of tungsten it would only be 40 W. Tungsten can also be utilized in the construction of magnets capable of generating permanent magnetic fields with inductions reaching several dozens of T. However, to achieve this, it would be necessary to connect a cryostat to a helium liquefier in order to reduce the cost associated with cooling such a magnet.

Autor: dr hab. inż. Stanisław Bednarek, Wydział Fizyki i Informatyki Stosowanej Uniwersytetu Łódzkiego, ul. Pomorska 149/153, 90-236 Łódź, E-mail: stanislaw.bednarek@fis.uni.lodz.pl

REFERENCES

- [1] Duncan R.C., Thompson Ch., Formation of very strongly magnetized neutron stars: Implications for gamma-ray bursts, *Astrophysical Journal Letters*, 392 (1992), 1, L9-L13
- [2] Treumann R.A., Baumjohann W., Balogh A., The strongest magnetic fields in the universe: how strong can they become?, *Frontiers in Physics*, 2, (2014), 1-4, doi: 10.3389/fphy.2014.00059
- [3] Kuwahata A., Kitaizumi T., Saichi K., Sato T., Igarashi R., Ohshima T., Masuyama Y., Iwasaki T., Hatano M., Jelezko F., Kusakabe M., Yatsui T., Sekino M., Magnetometer with nitrogenvacancy center in a bulk diamond for detecting magnetic nanoparticles in biomedical applications, *Scientific Reports*, 10 (2020), p. 2483-2492, doi.org/10.1038/s41598-020-59064-6
- [4] Hong-Chang Y., SQUID: The most sensitive detector of magnetic flux, *Tamkang Journal of Science and Engineering*, 6 (2003), 1, p. 9-18
- [5] Kominis I.K., Kornack T.W., Allred J.C., Romalis M.V., A subfemtotesla multichannel atomic magnetometer, *Nature*, 422, (2003), p. 596-599
- [6] Griffith W.C., Knappe S., Kitching, K., II. *Optical. Express*, 18, (2010), p. 27167-27172
- [7] Wu Chao A., Mess K.H., Tinger M., Zimmermann F., *Handbook of Accelerators Physics and Engineering*, World Scientific (2013)
- [8] Truck B., Tore supra: A tokamak with superconducting toroidal field coils, *IEEE Transaction on Magnetism*, 25 (1989), p. 1473-1480
- [9] N'gotta P., Le Beck G, Chavanne J., Hybrid high gradient permanent magnet quadrupole, *Physical Review of Accelerator Beams*, 19 (2016), p. 122-124
- [10] Klitzing K., Quantum Hall Effect: Discovery and Application, *Annual Review of Condensed Matter Physics*, 8, (2017), p. 13-20, doi.org/10.1146/annurev-conmatphys-031016-025148
- [11] Motokawa M., Watanabe K., Awaji S., High magnetic field research in Tohoku University, *Current Applied Physics*, 3 (2003), p. 367-376
- [12] Lubkin G.B., Florida dedicated National High Magnetic Field Laboratory, *Physics Today*, 12 (1994), p. 21-23
- [13] Herlach J.F., Miura N. (Editors), *High Magnetic Fields Science and Technology, Vol. 2, Theory and Experiments I*, World Scientific (2003)
- [14] Nakamura D., Record indoor magnetic field of 1200 T generated by electromagnetic flux-compression, *Review of Scientific Instruments*, 89 (2018), 9, p. 095106, doi: 10.1063/1.5044557
- [15] Nojiri H., Takamasu T., Todo S., Uchida K., Haryama T., Katori H.A., Goto T., Miura N., Generation of 500 T fields by electromagnetic flux compression and their application to cyclotron resonance, *Physica B* 201 (1994), p. 579-583
- [16] Kane B.E., Dzurak A.S., Facer G.R., Clark R.G., Starrett R.P., Skougarevsky A., Lumpkin N.E., Measurement instrumentation for electrical transport experiments in extreme pulsed magnetic fields generated by flux compression, *Review of Scientific Instruments*, 69 (1997), 10, p. 3843-3860
- [17] Knoepfel H., *Pulsed High Magnetic Fields, Physical Effects and Generation Methods Concerning Pulsed Fields up to the Megaersted Level*, Nord-Holland Publishing Company, (1970)
- [18] Ding H., Yuan Y., Xu Y., Jiang C., Li L., Duan X., Pan, J. Hu J., Testing and Commissioning of a 135 MW Pulsed Power Supply at the Wuhan National High Magnetic Field Center, *IEEE Transaction on Applied Superconductivity*, 24 (2014), p. 3, doi:10.1109/TASC.2013.2292305
- [19] Cyrot M., Pavuna D., Introduction to Superconductivity and High T_c Materials, World Scientific Publishing Co. (1992)
- [20] Motokawa M., Nojiri H., Tokunaga Y., An idea for the easy construction of a high field magnet, *Physica B*, 155 (1989), p. 96-99
- [21] Peng T., Jiang F., Sun Q.Q., Pan Y., Herlach F., Li L., Concept Design of 100 T Pulsed Magnet at the Wuhan National High Magnetic Field Center, *IEEE Transaction on Applied Superconductivity*, 26, (2014), p. 4, doi: 10.1109/TASC.2015.2523366
- [22] Back C.H., Siegmann H.C., Ultrashort magnetic field pulses and elementary process of magnetization reversal, *Journal of Magnetism and Magnetic Materials* 200 (1999), p. 774-785
- [23] Siegmann H.C., Magnetism in the picosecond time scale with electron accelerators, *Europhys. News*, 31 (2000), 6, p. 24-25
- [24] Mackay K., Bonfim M., Givord D., Fontaine A., 50 T pulsed magnetic fields in microcoil, *Journal of Applied Physics*, 87, (2000), 4, p. 1996-2002
- [25] Desai E., Electrical resistivity of tungsten, *Journal of Physical Chemistry, References. Data*, 13 (1984), 4, p. 1091-1096
- [26] Haynes W.M., (Editor in Chief), *CRC Handbook of Chemistry and Physics*, CRC Press Taylor and Francis Group (2017)
- [27] Bitter F., The design of powerful electromagnet, Part. II. The magnetizing coil, *Review of Scientific Instruments*, 7 (1936), 482-489
- [28] Herlach J.F., Miura N., (Editors), *High Magnetic Fields Science and Technology, Vol. 1, Magnet Technology and Experimental Technique*, World Scientific, (2003)